Proceedings of the 6th International Conference of Fluid Flow, Heat and Mass Transfer (FFHMT'19)
Ottawa, Canada – June, 2019
Paper No. FFHMT 145
DOI: 10.11159/ffhmt19.145

Maximizing Mass Transfer Using Highly Curved Helical Pipes: A CFD Investigation

Omran Abushammala, Rainier Hreiz, Cécile Lemaître, Éric Favre
Laboratoire Réactions et Génie des Procédés
Université de Lorraine, CNRS, LRGP
F-54000 Nancy, France
Omran.abushammala@univ-lorraine.fr; Rainier.hreiz@univ-lorraine.fr; Cecile.lemaitre@univ-lorraine.fr;
Eric.favre@univ-lorraine.fr

Abstract - Membrane contactors are considered as one of the most promising intensification technologies for gas-liquid absorption processes in food, chemistry, energy and pharmaceutical industries. Two strategies can be applied in order to push process intensification: maximize mass transfer coefficients and maximize the specific membrane surface area (i.e. packing density) of the module. Dean vortices generation is one of the most efficient way for mass transfer improvement but requires helical shape membranes. Consequently, a combined packing geometry and mass transfer study is needed in order to evaluate the optimal performances of helical hollow fiber membrane modules. This work aimed to achieve that target through a systematic analysis of mass transfer performances in highly curved hollow membrane contactors. The impact of the nondimensional numbers R_H^* , p^* (respectively the helical radius and helical pitch both nondimensionalized by the pipe diameter d) on mass transfer was evaluated numerically by using CFD. Helical hollow fiber membranes with lengths ranging from 30 to 6000 d, nondimensional helical diameters R_H^* between 0.05 and 10, and nondimensional helical pitches p^* between 1.25 and 15 were studied. In addition, mass transfer in packed membrane modules is analyzed thanks to a mass transfer enhancement factor ε, which is equal to the mass transfer ratio $Sh_H^\infty / Sh_S^\infty$ (comparing the Sherwood number of helical and straight pipes) multiplied by the packing density ratio Pa_H/Pa_{St} (comparing the packing density of helical and straight pipes). It is shown that enhancement is maximal for highly curved helical pipes. For example, for a Schmidt number of 10, highly curved pipes allow reaching a Sh_H^∞ value, which is about 4 times larger than that of a straight tube. For a Schmidt number 1000, the mass transfer efficiency can be enhanced by one order of magnitude.

Keywords: CFD, Dean vortices, Mass transfer, Intensification, Helical pipes, Packing density.

1. Introduction

Membrane separation is widely used for the separation of homogeneous liquid or gaseous mixtures, and is one of the most promising intensification technologies for gas-liquid absorption processes. The design and operation of membrane modules have been the focus of many scientific researches aiming to improve the separation efficiency. In this context, CFD (Computational Fluid Dynamics) proved to be a powerful tool to assist and support engineers in order to determine the optimal shape of membrane modules. Curved geometries are widely used in industrial processes and other applications since they exhibit secondary flows, in the shape of longitudinal vortices called Dean vortices, leading to much better performances than the straight pipes, Such geometries can be found in particular for: (1) Heat transfer enhancement with helically coiled heat exchangers commonly encountered in anaerobic digesters [1] refrigeration systems [2], power plants, and nuclear reactors [3] among many other applications; (2) Mass transfer enhancement in catalytic reactors [4], dense [5] and porous [6] membrane contactors, etc; (3) Fouling and clogging reduction in filtration membranes [7]; (4) Improvement of mixing efficiency and homogenization [8]. The present study addresses mass transfer in highly curved helical pipes, i.e. helical geometries with small helical radius and pitch. Figures 1 and 2 clarify why this shape is more efficient than the others.

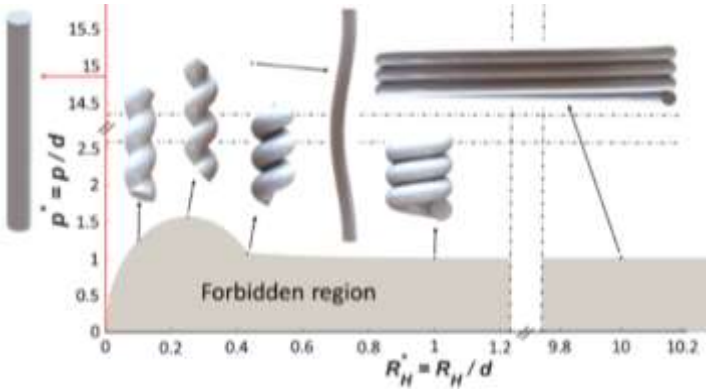

Fig. 1: Limits of the forbidden region in the (R_H^* , p^*) space (adapted from Przybył et.al [9]) and some representative helices.

Figure 1 presents the limits of the so-called forbidden region in the (R_H^* , p^*) space, where R_H^* and p^* are the reduced helix radius and pitch respectively, both nondimensionalized by the pipe diameter d. The forbidden region corresponds to the zone where it is not possible to design helical shapes. Its frontier, which equation has been determined by Przybył et.al [9], corresponds to closely packed helices, i.e. helices which pitch cannot be further decreased. Some helix designs are shown in Figure 1. They illustrate the fact that the helical pipe geometry tends toward that of a straight at three asymptotic limits: (i) when the dimensionless pitch p* tends to infinity; (ii) when the dimensionless helix radius R_H^* tends to infinity; (iii) when the dimensionless helix radius R_H^* tends to zero. Figure 2 shows the contours of the dimensionless helix curvature, κ*, in the (R_H^* , p^*) space. The dimensionless helix curvature κ*is equal to the of the ratio of d over γ, where γ is the radius of curvature of the helix. It appears in Figure 2 that the helix curvature tends to zero (equivalently that the radius of curvature tends to infinity) at the three asymptotic limits reported above. Moreover, the smallest curvature radii are associated to geometries with low pitches and relatively low helical radii. These geometries will be referred to as 'highly curved helical geometries' further on in this paper. Optimal helical membrane show the best trade-off between three parameters: the mass transfer expressed by the Sherwood number, the pressure drop characterized via the friction factor and the packing density. The pressure drop was investigated in a previous publication [10]in which a correlation for the ratio of fully developed friction factor in helical pipes Cf_H^∞ to straight ones, Cf_S^∞ (which equals 64/Re, following the Darcy-Weisbach definition) was proposed. As an example $Cf_H^\infty to\ Cf_S^\infty$ contours in the (R_H^* , p*) plane for a Reynolds number $Re = 400$, are reproduced in Figure 3, showing a maximum of $Cf_H^\infty to\ Cf_S^\infty$ for the maximum curvature κ*. The geometries with high curvatures investigated in the present communication are expected to produce the highest centrifugal effects, i.e. the most intense Dean vortices. However, to the authors knowledge, no study has considered yet the performance of such helical pipes, probably because they are difficult to manufacture using traditional

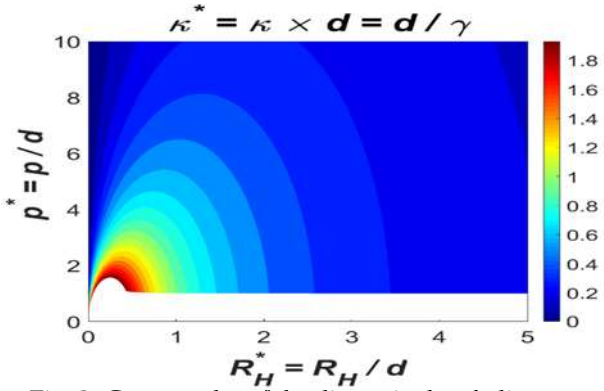

Fig. 2: Contour plot of the dimensionless helix curvature in the (R_H^*, p*) space.

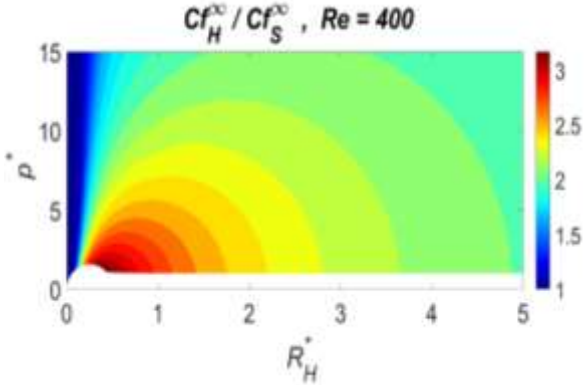

Fig. 3: Contour plot of the friction factor correlation at Reynold number=400.

techniques. However, nowadays, with the development of additive manufacturing and 3D printing technologies, the elaboration of highly curved helical geometries has become achievable. The following sections focus on mass transfer and packing density for different helical geometries. Computational fluid dynamics (CFD) simulations are carried out to determine the Sherwood number values in helical pipes. Different operating conditions, represented by the Reynolds and Schmidt numbers, and various helix designs, particularly highly curved helices, are examined. This study considers

laminar flow conditions only. Indeed, such a flow regime is commonly encountered in membranes, micro-structured heat exchangers and microfluidics applications, etc., due to the small scales of the employed devices.

2. Dimensional analysis and CFD modeling

2.1. Packing density

The packing density or compactness, Pa, represents the highest membrane volume (corresponding to the highest number of pipes) that can be packed within a unit volume of reactor. The ideal packing density is attained for the straight tube case $Pa_{St} = 90.7\%$. Kaufhold et al. [11] proposed the following equation for calculating the packing density of helical pipes:

$$\mathrm{Pa_H} = \frac{\pi}{4} 0.907 \frac{\left(2\mathrm{R_H} - \frac{\mathrm{d}}{2}\right)^2}{\left(2\mathrm{R_H} + \frac{\mathrm{d}}{2}\right)^2} \tag{1}$$

In this equation, the effect of the helix pitch was neglected. This hypothesis causes important errors in several situations. Indeed, the packing density should tend to $Pa_{St} = 90.7\%$. at two asymptotic limits: (i) when the dimensionless pitch p^* tends to infinity; (ii) when the dimensionless helix radius R_H^* tends to zero. Equation (1) fails to reproduce these limits.

In this paper, the packing density was computed mathematically and numerically using a CAD software. Assuming a triangular lattice disposition (i.e. hexagonal packing), A_{min} was determined for several helical geometries. A_{min} represents the minimum distance between two helix centres, under which the helix edges touch each other, as shown at Figure 4. Then, space is divided into periodic helices which cross-section is an equilateral triangle of side A_{min} which connects the centres of three neighbouring helices. This volume, $V_{\mathrm{triangular}}$, contains 1/6$^{\mathrm{th}}$ of all three helices, which corresponds to the volume of half a helix, $V_{half\ helix}$. The packing density of helical tube is the ratio of the volume of half helix to the triangular volume:

$$Pa_H = {V_{half\ helix}}\Big/{V_{triangular}} \tag{2}$$

$$V_{half\ helix} = \frac{\pi}{8} d^2 \sqrt{(2\pi R_H)^2 + p^2} \tag{3}$$

$$V_{triangular} = \frac{1}{2} A_{min}^2 \, sin(60°)\, p \tag{4}$$

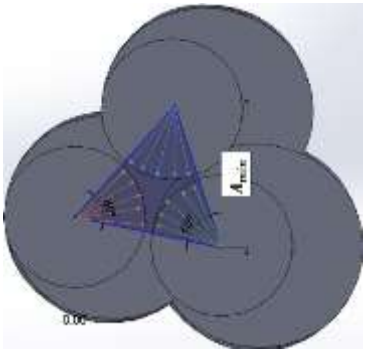

Fig. 4: The triangular shape from the three packed membranes.

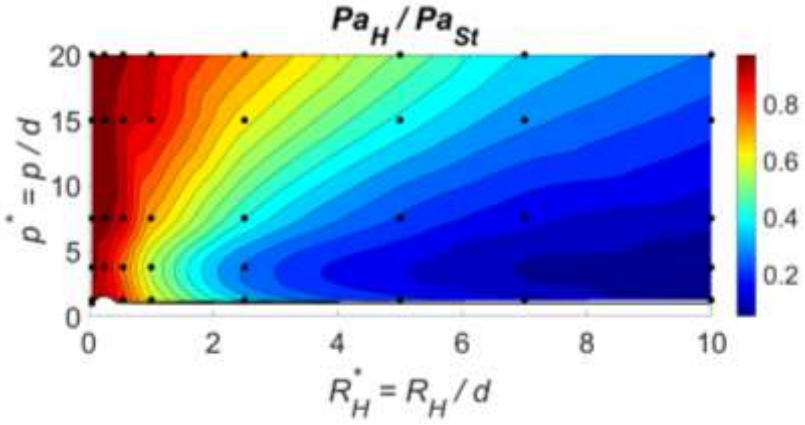

Fig. 5: Contour plots of Pa_H to Pa_{St} ratio at different helical geometries: data interpolated from CAD software results.

Figure 5 shows contour plots of the Pa_H to Pa_{St} ratio that were obtained using a triangulation-based cubic interpolation of CAD software results. The ratio Pa_H to Pa_{St} is inferior to one and increases when R_H^* decreases or p*

increases. It tends toward unity when R_H^* tends to zero or p* tends to infinity as the helix geometry approaches that of a straight pipe.

2.2. Sherwood number and dimensional analysis

In helical and curved pipes, the local mass flux across the wall and so the local Sherwood number are not uniform over the pipe. The Sherwood number is defined as

$$Sh = {}^{h_m d}/_{D_m} \tag{5}$$

where h_m and D_m are the mass transfer coefficient and mass diffusivity respectively. In most engineering applications, only the Sherwood number averaged over the pipe perimeter is of practical interest. Figure 6 illustrates a typical variation

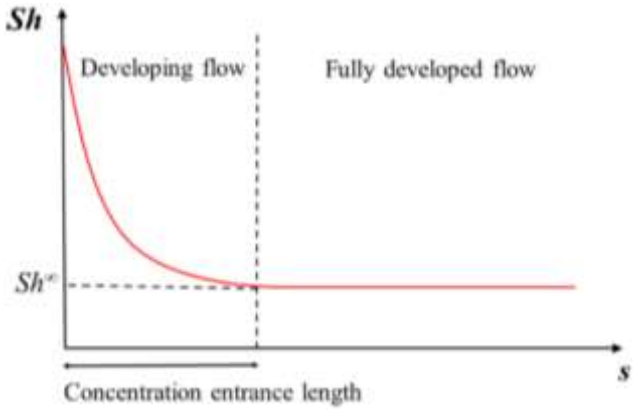

Fig. 6: Typical variation of the Sherwood number from the entrance of a straight or helical pipe.

of the perimeter-averaged Sherwood number along a helical or a straight tube, the abscissa axis being the curvilinear position along the pipe centreline. The Sherwood number is the highest at the pipe entrance and decreases over a distance called 'concentration entrance length' before reaching an asymptotic value, Sh^{∞}. Notations Sh_H^{∞} and Sh_S^{∞} will be used to designate the fully developed Sherwood number in helical and straight tubes respectively. If a uniform concentration is enforced at the wall, the theoretical value of Sh_S^{∞} is 3.65 for a straight tube. The equation describing mass transfer in a liquid medium is mathematically analogous to the heat transfer equation. Therefore, it is relevant to discuss mass and heat transfer in curved pipes simultaneously. Table. 1 shows the dimensionless relationships between heat and mass-transfer systems.

Table 1: Dimensionless groups for analogous heat and mass transfer systems.

Heat transfer	Mass transfer
Nusselt number $Nu = {}^{hd}/_{k}$	Sherwood number $Sh = {}^{h_m d}/_{D_m}$
Prandtl number $Pr = {}^{\vartheta}/_{\alpha}$	Schmidt number $Sc = {}^{\vartheta}/_{D_m}$

Where h, h_m, k, D_m, ϑ , α and d represent the heat transfer coefficient, mass transfer coefficient, thermal conductivity, mass diffusivity, kinematic viscosity, thermal diffusivity and diameter of the helical tube respectively. Therefore, according to the Buckingham-π theorem, the following four independent dimensionless parameters are required to correlate the Sh^{∞}data: (1) the dimensionless helix pitch, $p^* = p/d$ and (2) the dimensionless helix radius, $R_H^* = R_H/d$ which characterize the helix shape and (3) the Reynolds number, $Re = \rho u d/\mu$, which accounts for the operating conditions; (4) the Schmidt number, $Sc = {}^{\vartheta}/_{D_m}$, which is a dimensionless number defined as the ratio of momentum diffusivity (kinematic viscosity) to mass diffusivity.

2.3. Mesh-independence study

Flow simulations were conducted for various helical pipe with $1.25 \leq p^* \leq 15$ and $0.05 \leq R_H^* \leq 10$, and a Reynold number =400. The geometries were designed using Autodesk Inventor Professional 2018 software, considering a sufficient tube length to attain the fully developed flow region. The grid consisted of hexahedral cells only, with a boundary layer mesh in the near-wall zone for a more accurate calculation of the steep gradients prevailing in this zone. To check that the results are independent of the mesh resolution for each case, named A, B, C, and D a mesh-independence study was performed. Different meshes were considered, all consisting of hexahedral elements with significant refinement near the walls to allow capturing the thin concentration boundary layer. Average Sherwood result is used at mesh study, which it the average of Sherwood value from the membrane inlet until the plane which Sherwood will be infinity or fully develop. The results obtained with mesh A, B& C were very similar for all of the cases investigated as shown in in Table 2. Mesh model C was selected and used for all following simulation. Model C is a structural mesh with inflation layers 32 with first layer thickness $10^{-03} mm$ and edge sizing divisions numbers 80 and sweep division numbers 20 points per mm.

Table 2: Details of different grids used for the mesh-independence test.

Study case/Arc length 125mm	Number of cells	Average Sherwood number	Percentage change in Sherwood number %
Model A	23.8 Million	24.5	C & A =0.8%
Model B	12.6 Million	24.59	C & B = 0.5%
Model C	8.8 Million	24.7	
Model D	4.6 Million	25.5	C & D = 3%

2.4. CFD modeling and governing equations

Based on preliminary simulations, the cells size and density were chosen so at to ensure a mesh-independent solution. The commercial CFD package ANSYS (FLUENT 16.0) was used to simulate the hydrodynamics and mass transfer inside the helical pipe. A Newtonian incompressible fluid was considered, and the flow, treated as steady, laminar and isothermal, was described using the Navier-Stokes and continuity equations (6)- (8). The fluid physical properties, density and viscosity, were supposed constant and uniform: such an assumption is valid in the case of a dilute solutions, which is often the case in absorption applications. Following these assumptions, the hydrodynamics and mass transfer equations read:

$$div(\vec{v}) = 0 \tag{6}$$

$$\rho \overrightarrow{div}(\vec{v} \otimes \vec{v}) = -\vec{\nabla} p + \mu \vec{\Delta} \vec{v} \tag{7}$$

$$div(C\vec{v}) = D_m \nabla^2 C \tag{8}$$

where $\vec{v}$ is the velocity vector, μ the kinematic viscosity, p the pressure, ρ the density, C the concentration and D_m the mass diffusivity. As boundary conditions, a uniform velocity profile and a zero-concentration profile were set at the pipe inlet: as the flow rate is imposed, the gravity force has no effect on the flow field and therefore this body force term was not included in the Navier-Stokes equations. At the pipe outlet, a uniform pressure condition was used, and the no-slip and uniform concentration conditions were enforced at the pipe walls. The advective terms in Eqs. (6)- (8) were discretized with the Quadratic Upwind Interpolation of Convective Kinematics QUICK scheme while the diffusive ones were central-differenced. The momentum and energy equations were resolved using the Semi Implicit Method for Pressure-Linked Equations Consistent (COUPLED) algorithm. Pressure interpolation was carried out using a second order scheme. The convergence criteria required a decrease of at least 10 orders of magnitude for the residuals.

3. Results and discussion

As mentioned earlier, for each simulation performed, the circumference-averaged Sherwood number was calculated at different positions across the pipe length so as to determine its asymptotic value Sh_H^∞ in the fully developed flow region. Figure 7 show the contour plot of $Sh_H^\infty / Sh_S^\infty$ (ratio of the asymptotic Sherwood values for a helical and a straight pipe) for $\mathrm{Re} = 400$ and different Schmidt number values. The curves were obtained using a triangulation-based cubic

interpolation of the CFD results. The geometric parameters for which simulations were performed are represented by black dots. The accuracy of the values interpolated between these points depends on the interpolation scheme employed. Nonetheless, these contour plots allow deriving several major conclusions:

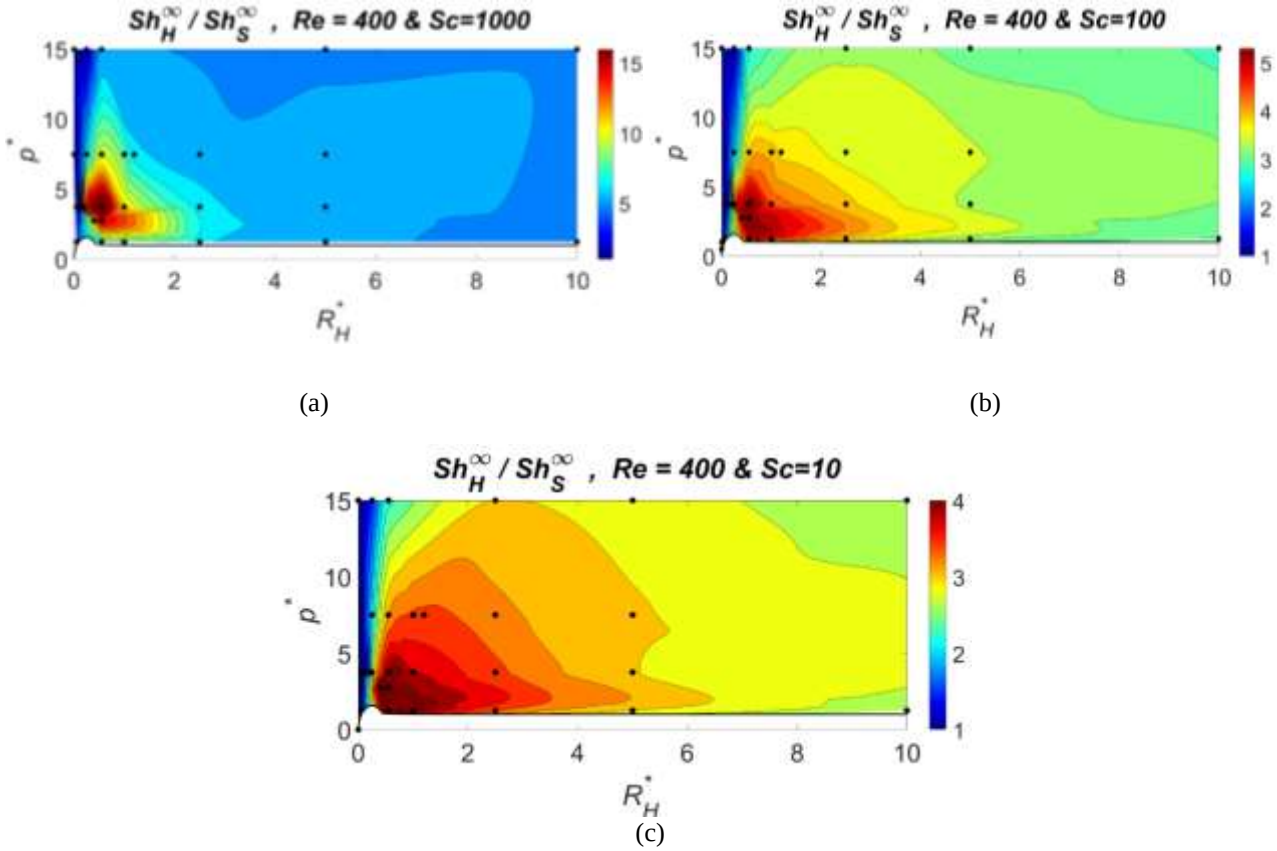

(a) (b)

(c)

Fig. 7: Contour plots of Sh_H^∞ to Sh_S^∞, ratio at different Schmidt numbers and a Reynold number equal to 400. The data is interpolated from CFD results marked with black dots. (a) *Sc*= 1000 (b) *Sc*=100 (c) *Sc*=10.

1- There is a positive correlation between Sh_H^∞ and the pipe curvature (Figure 2). Indeed, highly curved helices involve the highest Sherwood numbers, which is explained by the fact that they engender the most intense Dean-type recirculations.

2- For each dimensionless pitch, p^*, there exists a dimensionless helical radius, R_H^*, at which the Sherwood number is maximal. The ratio Sh_H^∞/Sh_S^∞ tends to one when R_H^* tends to zero or infinity, since the helical geometry approaches that of a straight pipe.

3- The mass transfer efficiency is extremely sensitive to the pitch value in the case of high curved helixes. For an infinite pitch, Sh_H^∞/Sh_S^∞ tends to one since the helical geometry tends to a straight pipe.

4- In addition, increasing the Schmidt number leads to an enhancement of the mass transfer for all helical and straight tubes. And the enhancement is the highest for highly curved helical pipes. For example, for a *Sc* of 10 high curved pipes allow reaching a Sh_H^∞ value is about 4 times than in straight tube. For a *Sc* of 1000, the mass transfer efficiency is enhanced by one order of magnitude.

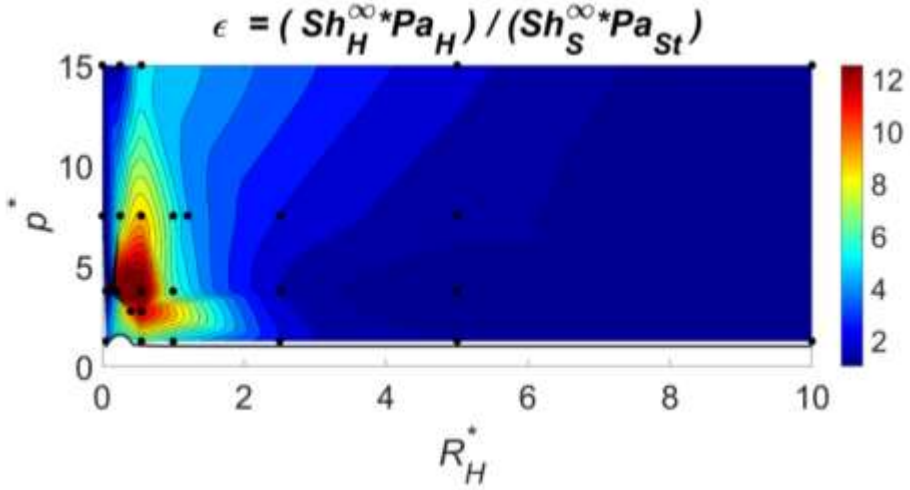

Fig. 8: The mass transfer enhancement factor ε at *Re* = 400 and *Sc* = 1000.

Finally, the enhancement factor ε, which is defined as the mass transfer ratio of helical and straight tubes multiplied by the packing density ratio, is considered

$$\varepsilon = \frac{Sh_H^{\infty}}{Sh_S^{\infty}} \frac{Pa_H}{Pa_{St}} \tag{9}$$

Figure 8 shows the contour of ε for Reynold number 400 and Schmidt number 1000. The highly curved helical geometries show an enhancement factor ε up to 12 times higher than the straight tube, which confirms the efficiency of these geometries. So despite the fact that helical membranes cannot be as densely packed than straight ones, they allow increasing the global mass transfer efficiency by an order of magnitude. Some previous studies (e.g. [11]) have come to the opposite conclusion as they only considered helixes with large helical radiuses on the one hand, and because of an imprecise computation of the helixes packing density on the other hand.

4. Conclusions

In this paper, the mass transfer across the wall of highly curved helical pipes was investigated numerically, by computing the Sherwood number Sh_H^{∞} and packing density Pa_H. This study demonstrates that these geometries allow a great enhancement of the mass transfer rate. For example with a Sc about 1000 (which corresponds to gas absorption processes), the achieved mass transfer efficiency is an order of magnitude higher than in classic membrane contactors. In a previous study [10], the pressure drop in highly curved geometries was investigated both numerically and experimentally. In the future, mass transfer experiments will be performed for such geometries, in order to validate the numerical results. After validation, correlations will be proposed to predict heat and mass transfer efficiency in helical pipes. These correlations will be used in model-based optimization of helically coiled heat exchangers/membrane contactors to determine the optimal helix geometry, i.e. the one leading to the most lucrative trade-off between the transfer efficiency enhancement and the increase of pumping costs.

References

[1] L.Yanfeng, Y. Chen, Y. Zhou, D. Wang, Y. Wang, and D. Wang, "Experimental research on the thermal performance of PEX helical coil pipes for heating the biogas digester," *Applied Thermal Engineering*, vol. 147, pp. 167-176, 2019.

[2] G. Jatinder, and J. Singh, "Use of artificial neural network approach for depicting mass flow rate of R134a/LPG refrigerant through straight and helical coiled adiabatic capillary tubes of vapor compression refrigeration system," *International Journal of Refrigeration*, vol. 86, pp. 228-238, 2018.

[3] I. Pioro, *Handbook of Generation IV Nuclear Reactors*. Woodhead Publishing, 2016.

[4] M. H. Abdel-Aziz, I. A. S. Mansour, and G. H. Sedahmed, "Study of the rate of liquid–solid mass transfer controlled processes in helical tubes under turbulent flow conditions," *Chemical Engineering and Processing: Process Intensification*, vol. 49, pp. 634-648, 2010.

[5] D. L. M. Mendez, C. Lemaitre, C. Castel, M. Ferrari, H. Simonaire, and E. Favre, “Membrane contactors for process intensification of gas absorption into physical solvents: Impact of dean vortices,” *Journal of Membrane Science*, vol. 530, pp. 20-32, 2017.
[6] R. Ghidossi, D. Veyret, and P. Moulin, “Computational fluid dynamics applied to membranes: State of the art and opportunities,” *Chemical Engineering and Processing: Process Intensification,* vol. 45, pp. 437-454, 2006.
[7] R. Moll, D. Veyret, F. Charbit, and P. Moulin, “Dean vortices applied to membrane process: Part I. Experimental approach,” *Journal of Membrane Science,* vol. 288, pp. 307-320, 2007.
[8] M. Mansour, Z. Liu, G. Janiga, K. Nigam, K. Sundmacher, D. Thévenin, and K. Zähringer, “Numerical study of liquid-liquid mixing in helical pipes,” *Chemical Engineering Science,* vol. 172, pp. 250-261, 2017.
[9] S. Przybył, and P. Pierański, “Helical close packings of ideal ropes,” *The European Physical Journal E,* vol. 4, pp. 445-449, 2001.
[10] O. Abushammala, R. Hreiz, C. Lemaître, E. Favre, “Laminar flow friction factor in highly curved helical pipes: numerical investigation, predictive correlation and experimental validation using a 3D-printed model,” submitted to *Chemical Engineering Sciences*, 2019.
[11] D. Kaufhold, F. Kopf, C. Wolff, S. Beutel, L. Hilterhaus, M. Hoffmann, T. Scheper, M. Schlüter, and A. Liese, “Generation of Dean vortices and enhancement of oxygen transfer rates in membrane contactors for different hollow fiber geometries,” *Journal of Membrane Science*, vol. 423, pp. 342-347, 2012.